S-adenosylmethionine addiction confers sensitivity to methionine restriction in *KMT2A*-rearranged acute lymphoblastic leukemia

Trisha Tee,[1] Titine J.J. Ruiter,[2+] Shuiyan Wu,[3+] Weiya Zhang,[1+] Dorette van Ingen Schenau,[1] Maria Rodionova,[1] Danique Wajon,[1] Britt M.T. Vervoort,[1] Kari J.T. Grünewald,[1] Marjolein Bosma,[2] Rico Hagelaar,[1,4] John Baker-Hernandez,[1] Ahmed Dahaoui,[1] Pauline Schneider,[1] Nanda M. Verhoeven-Duif,[2] Laurens T. van der Meer[1#] and Frank N. van Leeuwen[1#]

[1]Princess Máxima Center for Pediatric Oncology, Utrecht, the Netherlands; [2]Department of Genetics, Metabolic Diagnostics, UMC Utrecht, Utrecht, the Netherlands; [3]Department of Hematology and Oncology, Children's Hospital of Soochow University, Suzhou, China and [4]Oncode Institute, Utrecht, the Netherlands

[+]*TJJR, SW and WZ contributed equally.*
[#]*LTvdM and FNvL contributed equally as senior authors.*

Correspondence: F.N. van Leeuwen
f.n.vanleeuwen@prinsesmaximacentrum.nl

Received: December 15, 2023.
Accepted: April 14, 2025.
Early view: April 24, 2025.

https://doi.org/10.3324/haematol.2023.284869

Abstract

Current intensive chemotherapy regimens have improved overall survival in pediatric acute lymphoblastic leukemia (ALL) but fail to cure some high-risk patient subgroups. We observed that lysine methyltransferase 2A-rearranged (*KMT2A-r*) leukemia, an aggressive subset with a dismal prognosis, is particularly vulnerable to perturbations of the methionine cycle. We demonstrate that this methionine dependency is driven by an increased need for S-adenosylmethionine (SAM) to maintain the hypermethylated state of *KMT2A-r* leukemias. Important pro-survival *KMT2A-r* target genes are repressed under methionine restriction, which, combined with other downstream metabolic changes, results in rapid cell death. FIDAS-5, an orally active methionine adenosyltransferase 2A (MAT2A) inhibitor that blocks SAM production, successfully impaired leukemia progression in patient-derived xenograft models, and a drug screen revealed strong synergy between MAT2A inhibition and histone deacetylase inhibitors. Our results identify the methionine cycle as a targetable vulnerability in *KMT2A-r* leukemia, which may increase the efficacy of epigenetic targeting agents.

Introduction

Lysine methyltransferase 2A-rearranged (*KMT2A-r*) acute lymphoblastic leukemia (ALL), also known as mixed-lineage leukemia (MLL)-rearranged ALL, accounts for 5% of childhood ALL cases, primarily affecting infants.[1] Though many young patients experience initial remission, their high relapse rate leads to a dismal 50% overall survival.[2] This underscores the urgent need for more effective therapies. Cancer cells rely heavily on exogenous nutrients to sustain rapid growth. ALL leukemic blasts for example, lack significant expression of asparagine synthetase, causing a dependence on extracellular asparagine.[3] Consequently, the use of asparaginase has become a cornerstone of the pediatric ALL treatment protocol and one of the most successful amino acid therapies in cancer to date. Other avenues for targeting metabolic dysregulation include glutamine dependence in glioma, breast, and prostate cancer, and altered branched-chain amino acid and serine metabolism.[4-6]

Methionine dependence in cancer cells was first observed in the 1970s,[7] and dietary methionine restriction (MR) and the use of methioninase, an enzyme that degrades methionine, have shown promising anticancer effects.[8-10] We explored the efficacy of MR in B-cell progenitor ALL (BCP-ALL) and observed a high sensitivity to methionine cycle disruption in *KMT2A-r* ALL. Methionine is an essential amino acid and is an important precursor to S-adenosylmethionine (SAM), the universal methyl donor for all methylation reactions. Our study indicates that *KMT2A-r* ALL is uniquely sensitive to MR due to its dependence on SAM. *KMT2A* encodes a histone methyltransferase that, when translocated, promotes leukemogenesis through off-target histone methylation and changes in gene expression.[11] The KMT2A fusion complex requires more SAM to maintain this hypermethylated state, creating a tar-

getable metabolic vulnerability in these young *KMT2A-r* ALL patients.

Methods

Ethical statement

Patient-derived xenografts (PDX) were generated from patient enrolled in trials upon treatment of pediatric ALL conducted by individual member groups of the International BFM study group: the AIEOP-BFM study group (Austria, Germany, Italy, and Switzerland), the FRALLE study group (France), the United Kingdom (UK) National Cancer Research Institute Childhood Cancer and Leukemia group, and the Dutch Childhood Oncology group. All treatment trials were approved by the respective national institutional review boards, and informed consent for the use of spare specimens for research was obtained from the study individuals, parents, or legal guardians.

Cell viability and metabolic activity assays

Cell viability was determined using amine staining (LIVE/DEAD Fixable Dead Cell Stain Sampler Kit, Thermo Fisher Scientific, #L349630) according to the manufacturer's instructions. Metabolic activity was measured using MTT (Sigma-Aldrich, #475989) according to the manufacturer's instructions. Additional details can be found in the *Online Supplementary Appendix*.

Ex vivo culture of patient-derived xenografts

PDX were generated by intrafemoral injection of 1E6 viable primary ALL cells into NOD.Cg-PrkdcscidIl2rgtm1Wjl/SzJ (NSG) mice. The *ex vivo* co-culture has been described previously,[12] and additional details regarding the genetic background of the samples and the protocols can be found in *Online Supplementary Table S2* and the *Online Supplementary Appendix*.

Metabolic profiling

Metabolic profiling of 650 metabolites in NALM-6 and SEM cells was performed by Metabolon. Details regarding their procedures can be found in the *Online Supplementary Appendix*. Metabolites with a significant Log_2fold change of ±0.75 after 24 hours (h) MR were further analyzed using the Metaboanalyst 5.0 Pathway Enrichment program to determine enrichment of pathways defined in the Kyoto Encyclopedia of Genes and Genomes (KEGG).[13] Heatmaps were created using normalized values from Metabolon transformed into Z-scores and the pHeatmap package (RRID: SCR_016418).

Drug screen

Screening was performed at the high-throughput screening facility of the Princess Máxima Center. Cells were seeded in 384-well plates and treated with a 10-fold dilution series of each drug in the presence or absence of FIDAS-5 (MedChemExpress, #HY-136144) for 72 h. Cell viability was measured using an MTT assay. Details can be found in the *Online Supplementary Appendix*.

RNA sequencing

mRNA was isolated from triplicate samples using an RNeasy Mini Kit (Qiagen) before and after 24 h treatment with complete methionine depletion. Library preparation, sample sequencing, and data analysis, including differential gene expression analysis, were performed by NovoGene (Cambridge, UK). KEGG Enrichment analyses were performed using the Kyoto Encyclopedia of Genes and Genomes (KEGG) database.[14] Heatmaps were created using FPKM values transformed into Z-scores and the pHeatmap package (RRID: SCR_016418).

In vivo experiments

Animal experiments were approved by the Animal Experimental Committee of Radboud University (RU-DEC-2019-0036). Following engraftment, mice were randomized and treated as indicated. Tumor load was monitored by measuring the presence of leukemic blasts in the peripheral blood using flow cytometry. Circulating methionine was measured via hydrophilic interaction liquid chromatography as previously described.[15] Details can be found in the *Online Supplementary Appendix*..

Results

KMT2A-rearranged leukemias selectively undergo rapid apoptosis upon methionine restriction

To investigate the impact of MR on ALL, we cultured BCP-ALL cell lines with and without methionine. Notably, the absence of methionine induced considerably more cell death in *KMT2A-r* cell lines compared to non-*KMT2A-r* cells (Figure 1A; *Online Supplementary Figure S1A*). Expanding our analysis to include acute myeloid leukemia (AML) and T-ALL cell lines yielded a similar outcome (*Online Supplementary Figure S1B*). A dose titration of MR over time confirmed that *KMT2A-r* ALL cell lines require more methionine to survive. When the amount of methionine becomes limiting, viability of these cells rapidly decreased (Figure 1B; *Online Supplementary Figure S1C*) as measured by a loss of membrane integrity. Intriguingly, we observed no differences in metabolic activity responses to MR as measured by an MTT assay (Figure 1C; *Online Supplementary Figure S1D*). Both non-*KMT2A-r* and *KMT2A-r* cells halted metabolic activity in response to MR. Conversely, only *KMT2A-r* cells underwent rapid apoptosis (Figure 1D). Washout experiments further confirmed that non-*KMT2A-r* ALL cells resumed proliferation in normal growth medium, whereas *KMT2A-r* cell recovery was limited (*Online Supplementary Figure S2A*).

Dietary MR has shown promising antitumor effects in several cancer models, including recently in AML, underscoring its relevance in hematological malignancies.[16] We assessed the efficacy of a MR diet to reduce the *in vivo* expansion of

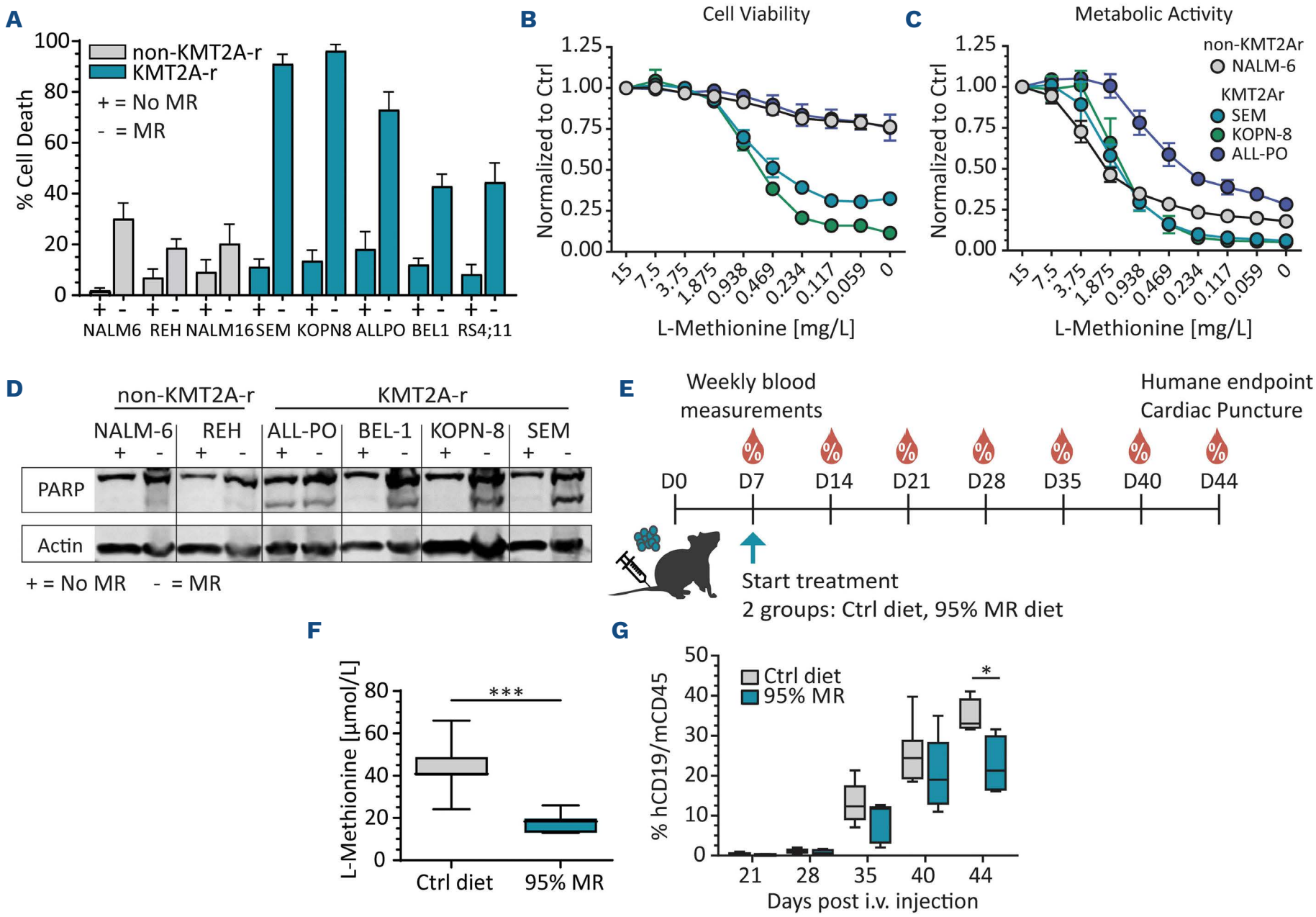

Figure 1. *KMT2A*-rearranged leukemias selectively undergo rapid apoptosis upon methionine restriction. (A) A panel of B-cell progenitor acute lymphoblastic leukemia (BCP-ALL) cell lines were treated with methionine-free RPMI1640 medium. Cell viability was measured after 72 hours (h) in 3 independent experiments. Values were normalized to the untreated controls (Ctrl). Non-normalized values can be found in *Online Supplementary Figure S1B*. Error bars represent standard deviation (SD) of biological replicates. (B) Dose response of several BCP-ALL cell lines to decreasing amounts of methionine in RPMI1640 medium. Cells were treated for 48 h before cell viability was measured by flow cytometry. Results shown are corrected to the viability of the untreated cells and represent the mean ± SD from 3 independent experiments. (C) Dose response of the same BCP-ALL cell lines performed in parallel using metabolic activity (MTT) as a read-out after 48 h. Results shown are corrected to the fluorescence of the untreated cells and represent the mean ± SD from 3 independent experiments. (D) Western blot showing PARP cleavage in lysates of cells after complete methionine depletion for 48 h. Similar results were observed in 2 independent experiments. (E) Timeline of the *in vivo* experiment performed in NSG mice injected with SEM cells. One week after engraftment, mice were randomly assigned to either a control diet (N=7) or a 95% methionine restriction (MR) diet (N=7) and kept on this diet until the humane endpoint was reached. Leukemia progression was monitored weekly by flow cytometry. (F) Box plot indicating methionine levels measured in plasma after 6 weeks on a 95% MR diet (N=7). *P* value was calculated using a two-tailed unpaired *t* test (***$P<0.001$). (G) Disease progression measured by the percentage of human $CD19^+$ cells in the peripheral blood of mice treated with control diet (N=7) or 95% MR diet (N=7). *P* value was calculated using a mixed effects model assuming sphericity (*$P<0.05$). *KMT2A-r*: *KMT2A*-rearranged; i.v.: intravenous.

xenotransplanted *KMT2A-r* SEM cells. One week after transplantation, mice were assigned either a control or 95% MR diet, and tumor progression was monitored via flow cytometry (Figure 1E). A 6-week period on a MR diet effectively reduced plasma methionine levels by 59% (Figure 1F), which slowed leukemic growth by 35% (Figure 1G). Remarkably, mice on the 95% MR diet experienced no adverse effects, except for a 5% decrease in weight (*Online Supplementary Figure S2B, C*). Our findings show that pediatric *KMT2A-r* leukemia is highly dependent on methionine for cell survival, which can be exploited using dietary MR.

Global metabolomics reveals that non-*KMT2A*-rearranged and *KMT2A*-rearranged cells have different metabolic landscapes

To further explore the differences in the response to MR, we performed bulk RNA sequencing on non-*KMT2A-r* NALM-6 and *KMT2A-r* SEM cells before and after 24 h of complete

MR. Looking at global changes, we observed an overall greater effect of MR on gene regulation in NALM-6 cells than in SEM cells, with 1,429 total differentially expressed genes compared to 707, respectively (Figure 2A; *Online Supplementary Figure S3A*). SEM cells showed a relatively even split between upregulated and downregulated genes, whereas NALM-6 cells exhibited more downregulated than upregulated genes, which aligns with our hypothesis that these cells may enter a state of quiescence. Only 20% of the upregulated and downregulated genes in NALM-6 cells overlapped with the respective upregulated and downregulated genes in SEM cells indicating clear differences in response upon MR treatment. Ranked KEGG enrichment analysis highlighted several metabolic pathways (in bold) that were regulated differently between cell lines after MR, including folate biosynthesis, sugar metabolism, and several amino acid metabolism pathways (Figure 2B). These results demonstrate the impact of MR on global metabolic function and suggest that differential sensitivity to MR may be determined by metabolic adaptation capabilities.

To explore this further, we performed global metabolomics using the same leukemic cell models. We evaluated 650 known metabolites before and after 12 h and 24 h of complete MR. Using unsupervised clustering, we observed clear differences both during steady state and after treatment (Figure 2C). Principal component analysis revealed strong segregation between the control and treated cells for both leukemias (*Online Supplementary Figure S3B*). Analysis of variance (ANOVA) contrasts were used to identify significantly different metabolites among the experimental groups (*Online Supplementary Table S1*). Over 400 metabolites showed contrasting concentrations at baseline, underscoring the metabolic uniqueness of each leukemia. MR had a significant impact on both cell lines, affecting approximately two-thirds of all measured metabolites. We used Metaboanalyst 5.0[13] for KEGG enrichment analysis of differential metabolites after 24 h of MR. This revealed pyrimidine metabolism as the most differentially enriched pathway in SEM cells (Figure 2D; *Online Supplementary Figure S3C*). We observed increased amounts of pyrimidines, uracil and cytosine, at baseline in SEM compared to NALM-6, as well as more orotate and other key *de novo* pyrimidine synthesis intermediates (Figure 2E; *Online Supplementary Figure S3D*). We also saw an overall stronger decrease in these metabolites in SEM cells upon MR, suggesting that SEM cells have a more active pyrimidine metabolism than NALM-6 cells, and may depend on methionine to maintain this, a known function of methionine and the folate cycle.[17] We also drew parallels with our transcriptomics data and observed relatively unchanged expression of two essential rate-limiting enzymes of *de novo* pyrimidine synthesis in SEM cells after MR: carbamoyl-phosphate synthetase 2 (CAD) and dihydroorotate dehydrogenase (DHODH) (Figure 2F). On the contrary, in NALM-6 cells these enzymes were significantly downregulated after treatment. Excessive dependence on *de novo* pyrimidine synthesis has been observed before in *KMT2A-r* AML cells and identified as a therapeutic target.[18] To corroborate this, we performed a gene set enrichment analysis (GSEA) using transcriptomics data from a published cohort of 49 *KMT2A-r* patients and five non-*KMT2A-r* patients[19] and found that *KMT2A-r* patients were indeed enriched for pyrimidine metabolism genes (*Online Supplementary Figure S3E*). Furthermore, DHODH inhibition mitigated the effects of MR in SEM cells, while the effect in NALM-6 cells was minimal (Figure 2G; *Online Supplementary Figure S3F*). Taken together, our metabolomics and transcriptomics analyses show the comprehensive effects of MR on these cells and provide insight into an alternatively regulated metabolic network that may account for the increased methionine vulnerability in this subset.

KMT2A-rarranged leukemias are more dependent on S-adenosylmethionine than non-*KMT2A*-rearranged leukemias

To pinpoint key metabolites driving this differential sensitivity, we focused on the one-carbon cycle, a metabolic network driven by folate and methionine. This cycle not only feeds into pyrimidine metabolism, but also serves several important biological functions, including nucleotide and redox metabolism and lipid biosynthesis.[20] The folate and methionine cycles are interlinked by the rate-limiting enzyme methionine synthase (MTR), and are essential to produce SAM, the universal methyl donor (Figure 3A). Our metabolomics data revealed that one-carbon metabolism in NALM-6 and SEM cells responded differently to MR (Figure 3B). SEM cells exhibited a rapid increase in S-adenosylhomocysteine (SAH) and homocysteine after 12 h, likely due to methionine salvage, with fewer effects on other metabolites. In contrast, the one-carbon cycle in non-*KMT2A-r* NALM-6 cells was more globally affected by MR. We observed an overall increase in metabolites related to the folate cycle, the transsulfuration pathway, and polyamine synthesis. MR also had contrasting effects on one-carbon-related gene expression (*Online Supplementary Figure S4A*). Gene set enrichment analysis revealed a small but significant suppression of one-carbon metabolism genes in NALM-6 cells during MR, an effect not seen in SEM cells (*Online Supplementary Figure S4B*).

While basal intracellular methionine levels were similar between NALM-6 and SEM cells (Figure 3C, left), SEM cells showed almost 3-fold higher SAM levels (Figure 3C, right). As previously mentioned, SAM is the universal methyl donor for all methylation processes. The transfer of methyl groups from SAM is catalyzed by methyltransferases, a large group of SAM-dependent enzymes (Figure 3D).[21] In SEM cells, SAM levels dropped after MR, leading to decreased concentrations of several SAM-dependent enzyme-substrate complex products, including monomethylarsonate (MMA), dimethylarginine (DMA), creatine, and 5-methylcytosine

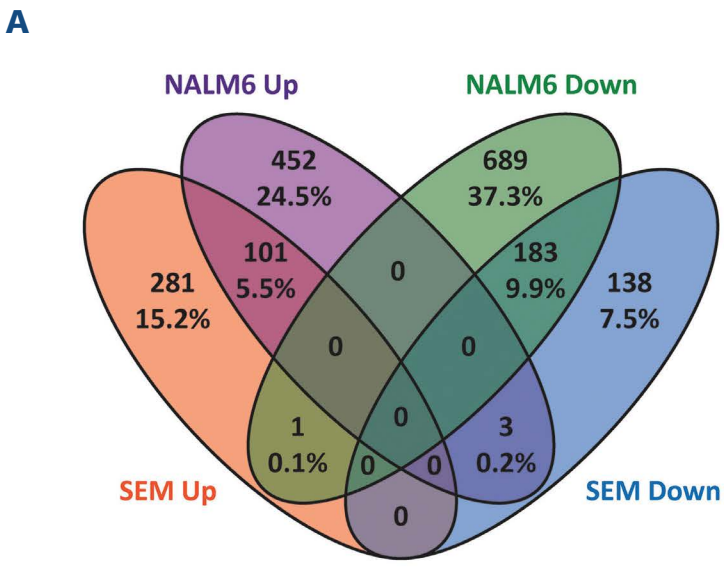

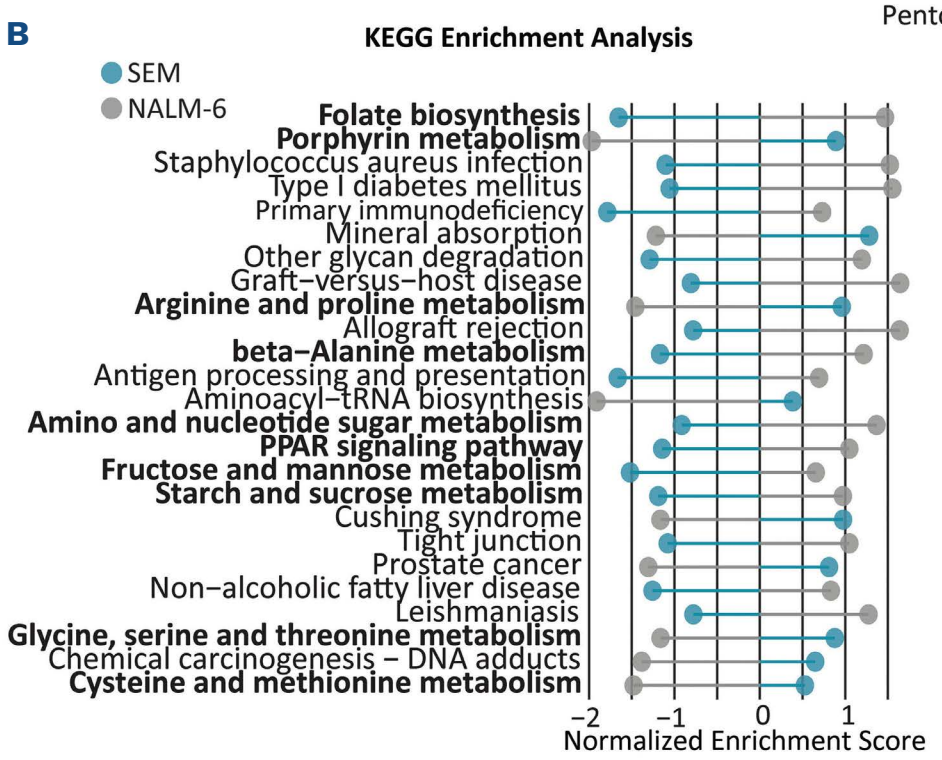

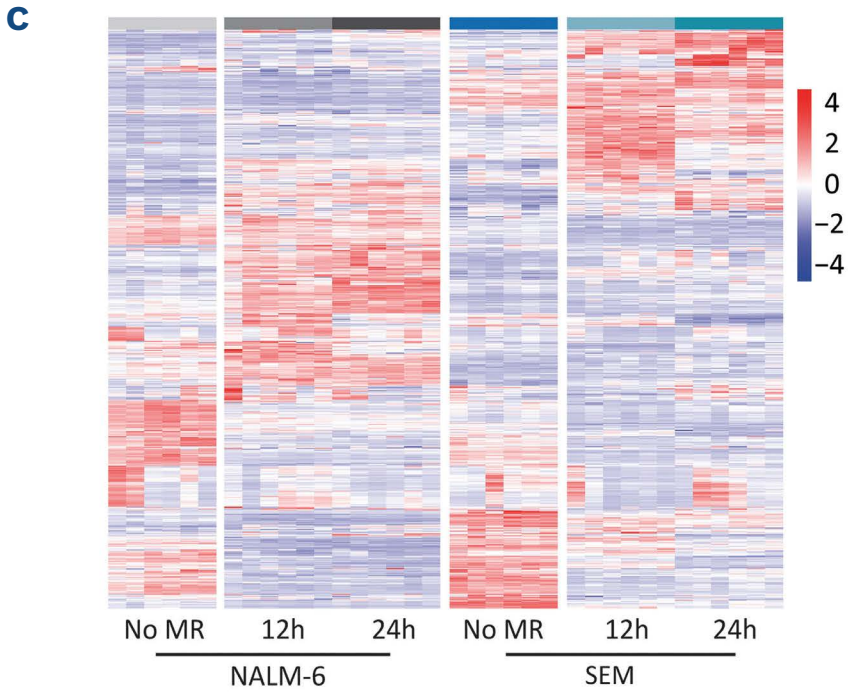

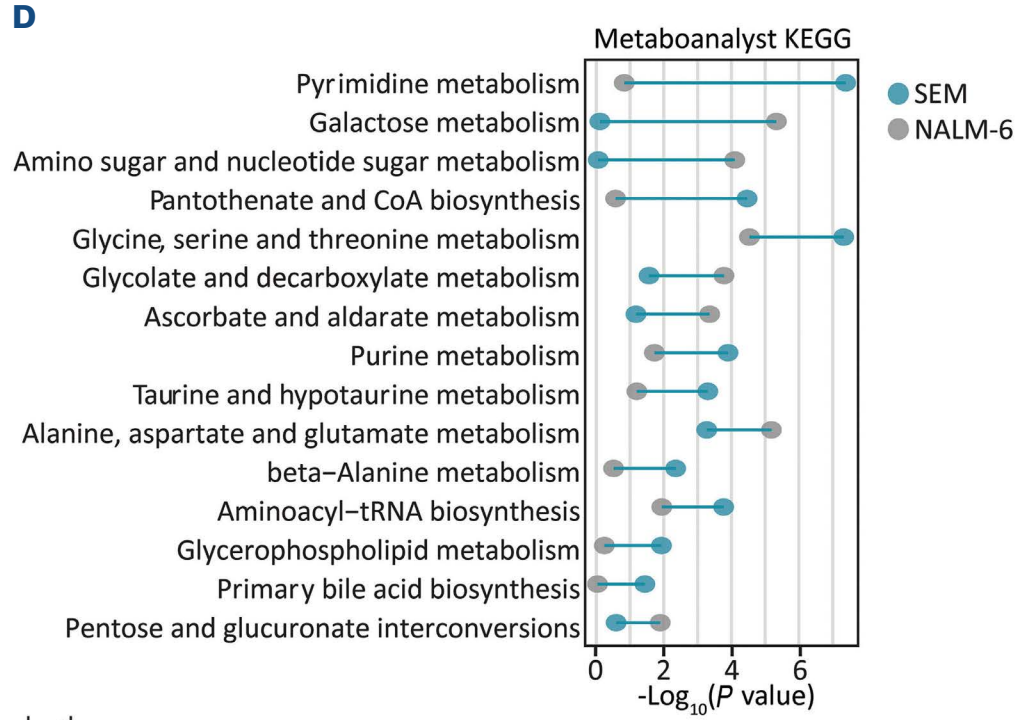

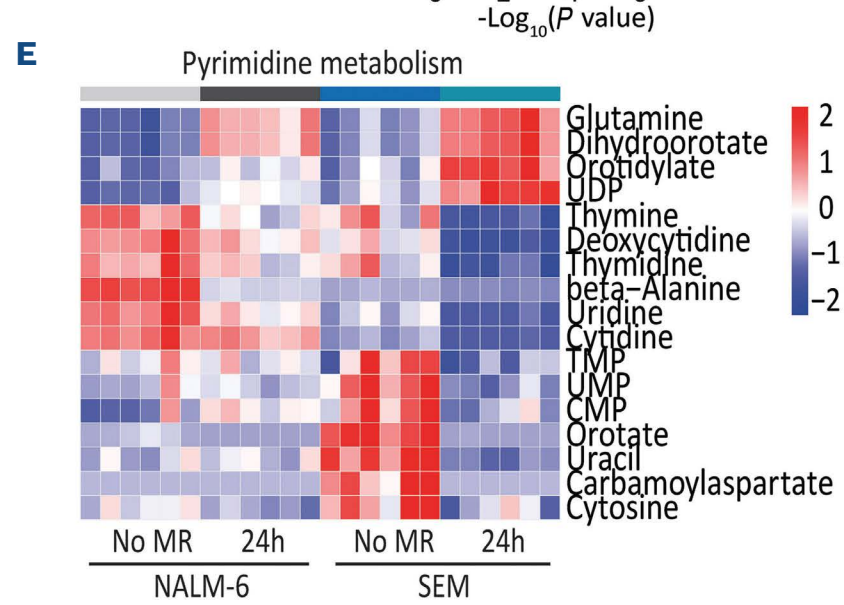

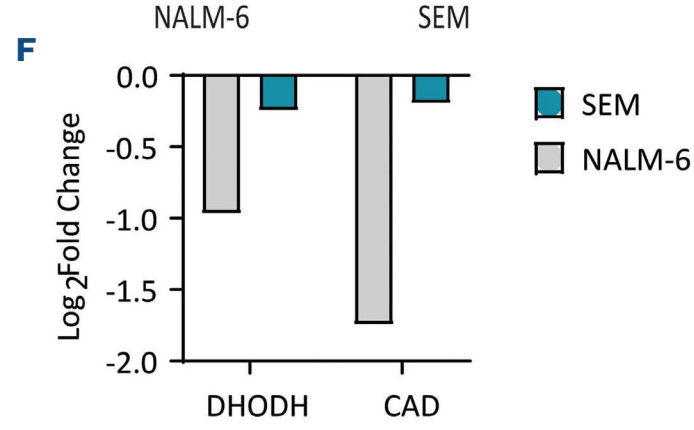

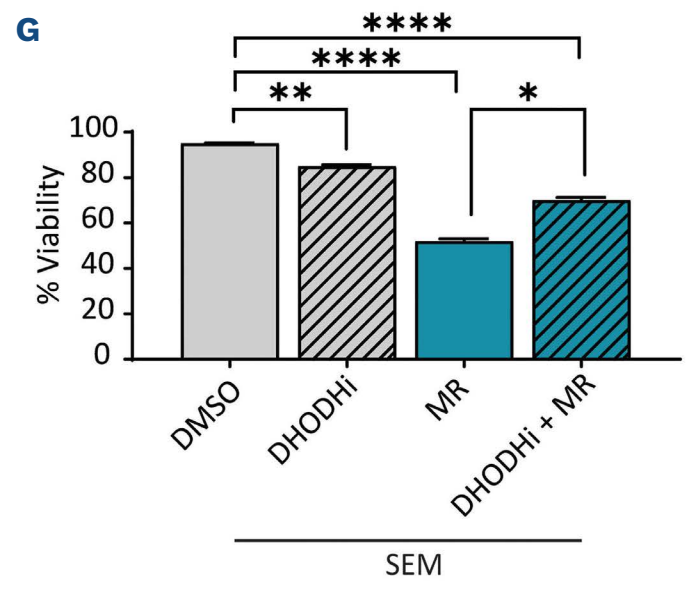

Continued on following page.

Figure 2. Global metabolomics reveals clear differences among metabolic processes between non-*KMT2A*-rearranged NALM-6 and *KMT2A*-rearranged SEM cells both at steady state and upon methionine restriction. (A) Venn diagram of the differentially expressed genes in NALM-6 and SEM cells. (B) Lollipop plot showing 25 KEGG pathways ranked from most to least different normalized enrichment scores between SEM (blue) and NALM-6 (gray) cells. Separate KEGG enrichment analyses were performed of the differentially expressed genes for each cell line using R. (C) Heatmap showing relative levels of 650 metabolites in non-*KMT2A*-rearranged (*KMT2A-r*) NALM-6 and *KMT2A-r* SEM cells treated with complete methionine depletion for 12 hours (h) or 24 h relative to their untreated controls. Global metabolomics was performed using services from Metabolon with 6 technical replicates per time point. (D) Lollipop plot showing 15 KEGG pathways ranked from largest to smallest difference in $-\text{Log}_{10}$(*P* value) between SEM (blue) and NALM-6 (gray) cells. Separate KEGG enrichment analyses were performed for each cell line using Metaboanalyst 5.0 software on metabolites with a log fold change of at least ±0.75 after 24 h MR (see *Online Supplementary Appendix*). (E) Sub-heatmap of pyrimidine metabolism pathway, showing unsupervised clustering of the relative levels of the specific metabolite hits from the KEGG enrichment analyses. (F) Log_2fold change in expression of dihydroorotate dehydrogenase (DHODH) and carbamoyl-phosphate synthetase 2 (CAD), obtained using RNA sequencing. (G) SEM cells were treated with 2 nM DHODH inhibitor, methionine restriction (MR) or the combination thereof for 72 h. Cell death was determined by quantification of cells positive for amine-reactive dyes using flow cytometry. *P* value was calculated using a one-way ANOVA and Dunnett's multiple comparison tests (*P<0.05; **P<0.01; ****P<0.0001).

(5-MC) (Figure 3E). This effect was less pronounced in NALM-6 cells (*Online Supplementary Figure S4C*). Expression of methyltransferases involved were also less affected in SEM cells upon treatment (Figure 3F; *Online Supplementary Figure S4D*), reinforcing the notion that despite amino acid stress and a shortage of SAM, *KMT2A-r* cells attempt to maintain normal one-carbon function.

We hypothesized from these analyses that MR is more consequential in *KMT2A-r* leukemia due to a greater need for SAM. Rescue experiments with SAM confirmed this, significantly inhibiting MR-induced cell death in *KMT2A-r* leukemic cell lines (Figure 3G). Furthermore, *KMT2A-r* cells displayed increased sensitivity to FIDAS-5, an inhibitor limiting SAM via targeting methionine adenosyltransferase 2A (MAT2A) (*Online Supplementary Figure S4E*). The same sensitivity was observed in PDX samples tested *ex vivo* (Figure 3H; *Online Supplementary Figure S4F*). These findings point to an increased SAM dependence in *KMT2A-r* ALL, making these leukemias more susceptible to methionine cycle perturbations, whether through dietary restrictions or targeted enzyme inhibition.

Methionine restriction suppresses global histone methylation in *KMT2A*-rearranged leukemias

Given the role of SAM in methylation reactions, we next explored the effects of MR on epigenetic modifications. An indicator of the capacity of cells to support methylation reactions, the methylation index is the ratio of SAM to SAH, where a decrease in this ratio predicts reduced cellular methylation potential. We noted that *KMT2A-r* SEM cells had a significantly higher methylation index compared to NALM-6 cells during steady state (Figure 4A). Consistent with the increased need for SAM, MR also resulted in a larger decrease in the methylation index in SEM cells. As a consequence, we observed rapid global suppression of major lysine methylation markers in *KMT2A-r* cell lines (Figure 4B), an effect that could be reverted by the addition of SAM (Figure 4C). In non-*KMT2A-r* cells, effect of MR on histone methylation was minimal. Intriguingly, effects on histone H3 lysine 4 (H3K4), lysine 79 (H3K79), and lysine 36 (H3K36), which are the modifications most associated with gene activation in *KMT2A-r* leukemia,[22-25] appeared to be most affected. This dependency on SAM to sustain the epigenetic state that drives tumor growth was previously noted in AML.[16] However, in contrast to AML, inhibition of lysine transferase SET domain containing 2 (SETD2) did not phenocopy methionine restriction in *KMT2A-r* ALL (*Online Supplementary Figure S5A*).

We next determined whether targeting demethylation of these specific modifications would affect sensitivity to MR and used interference RNA to suppress expression of lysine-specific demethylase 2B (*KDM2B*) in SEM cells. *KDM2B* is known for its preferential demethylation of H3K36 and H3K4[24,26] and has recently been shown to regulate H3K79.[27] *KDM2B* knockdown (KD) models exhibited significant resistance to MR compared to wild-type SEM cells (Figure 4D). Moreover, prolonged MR treatment favored outgrowth of cells with a more efficient knockdown (Figure 4E, right). A lysine-specific demethylase 4A (*KDM4A*) KD was also generated (*Online Supplementary Figure S5B*). *KDM4A* is specific for H3K9 methylation but can also demethylate H3K36 with lower efficiency.[28] We observed a similar MR-resistant phenotype with *KDM4A* KD (*Online Supplementary Figure S5C*), indicating that specific methylation marks may not solely determine MR sensitivity.

KMT2A-r leukemia relies on hypermethylation to activate target genes and drive aberrant growth. We therefore hypothesized that MR-induced demethylation triggers apoptosis by shutting down essential *KMT2A-r* target genes. Using a *KMT2A-AFF1* (*MLL-AF4*) target gene signature[29] (*Online Supplementary Figure S5D*), we observed strong effects of MR on SEM cells (Figure 4F). Although MR did not induce a global loss of the *KMT2A-AFF1* gene signature (*Online Supplementary Figure S5E*), several key *KMT2A-r* target genes that are known drivers of *KMT2A*-driven proliferation and survival, were significantly suppressed (Figure 4G). To further assess the effects of MAT2A inhibition on histone methylation, we used chromatin immunoprecipitation on H3K4 trimethylation, a modification affected by the MLL complex and associated with active transcription. Treat-

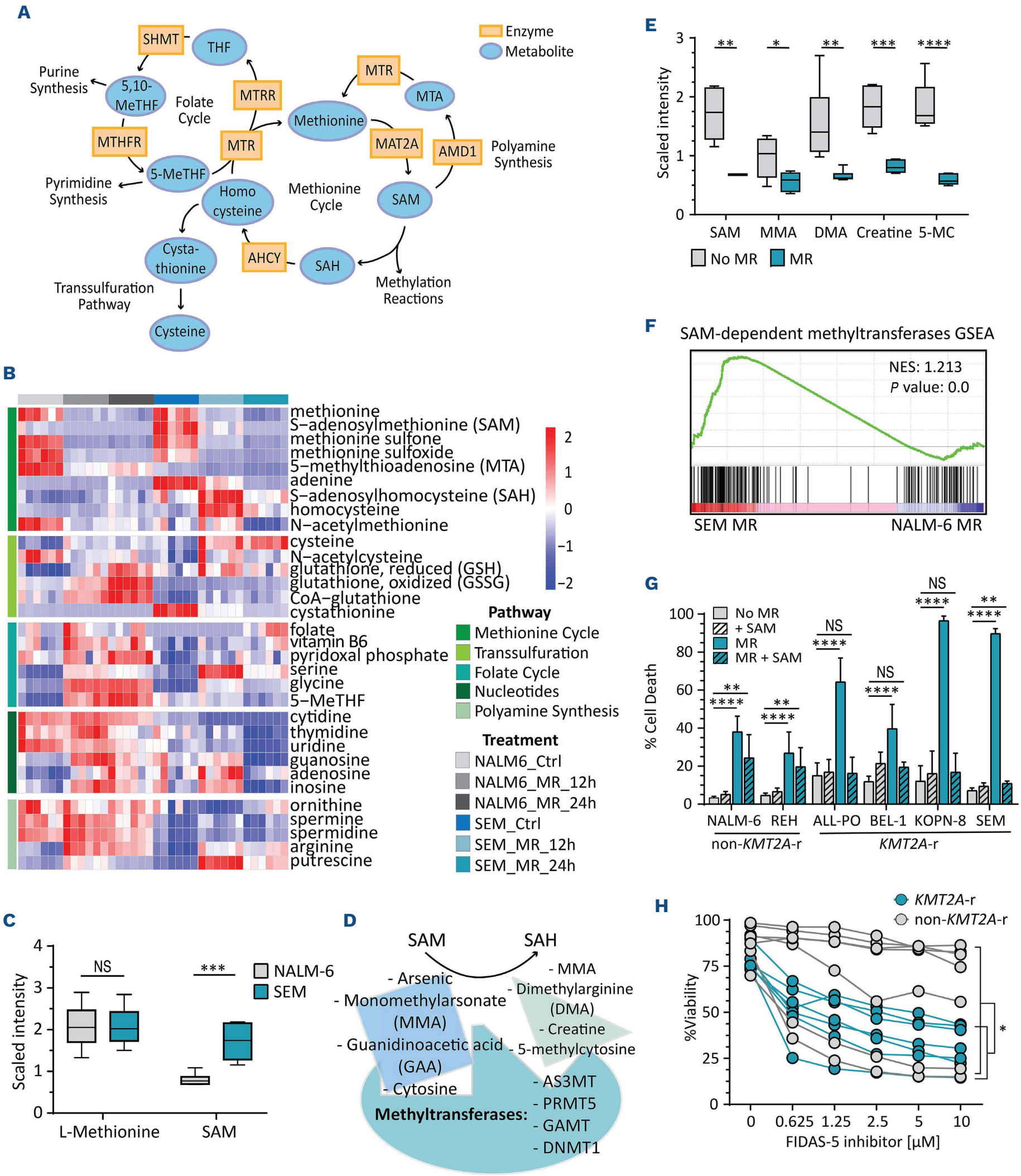

Figure 3. *KMT2A*-rearranged leukemias are uniquely dependent on S-adenosylmethionine, thereby creating a vulnerability to perturbations of the methionine cycle. (A) Schematic showing the methionine cycle and its central role in one-carbon metabolism, the transsulfuration pathway, and polyamine, purine, and pyrimidine synthesis. (B) Heatmap of metabolomics data showcasing key components of the methionine cycle and its linked pathways in NALM-6 and SEM cells at steady state, and 12 hours (h) and 24 h

Continued on following page.

after methionine depletion. (C) Box plots showing intracellular levels of L-methionine and S-adenosylmethionine (SAM) in NALM-6 and SEM cells. Values for each sample are normalized by Bradford protein concentrations and then re-scaled to set the median equal to 1. Calculations were performed as a service from Metabolon. *P* values were calculated using a two-tailed unpaired *t* test (****P*<0.001). (D) Schematic showing the substrates of different methyltransferases which utilize SAM to form their respective by-products. (E) Box plots of normalized and scaled levels, as calculated by Metabolon, of SAM and methyltransferase byproducts measured in SEM cells before and after 24 h complete methionine restriction (MR). *P* values were calculated using a two-tailed unpaired *t* test (**P*<0.05; ***P*<0.01; ****P*<0.001, *****P*<0.0001). (F) A Gene set enrichment analysis (GSEA) plot comparing MR treated SEM to treated NALM-6 cells using the gene ontology-based SAM-dependent methyltransferase gene set. (G) Rescue experiment performed by adding SAM back to MR medium and measuring cell viability 72 h later by flow cytometry. *P* value was calculated using a one-way ANOVA and Dunnett's multiple comparison tests (***P*<0.01; *****P*<0.0001). (H) Dose response of several B-cell progenitor acute lymphoblastic leukemia (BCP-ALL) patient-derived xenografts (PDX) to methionine adenosyltransferase 2A (MAT2A) inhibitor, FIDAS-5. Cells were seeded on a feeder layer of mesenchymal stem cells and treated for 72 h before measuring cell viability via flow cytometry. *P* value was calculated using a two-tailed unpaired Welch's *t* test of the area under the curves (AUC) comparing non-*KMT2A-r* PDX samples with *KMT2A-r* PDX samples. SHMT: serine hydroxymethyltransferase; MTHFR: 5,10-methylenetetrahydrofolate reductase; MTR: methionine synthase; MTRR: methionine synthase reductase; AMD1: adenosylmethionine decarboxylase 1; AHCY: adenosylhomocysteinase; THF: tetrahydroxyfolate; meTHF: methyl-tetrahydroxyfolate; MTA: methylthioadenosine; SAH: S-adenosyl-L-homocysteine; NS: not significant.

ment with MAT2A inhibitor FIDAS-5 for 24 h resulted in a reduction of H3K4 trimethylation, predominantly at transcription start sites (*Online Supplementary Figure S6A*). The affected genes (*Online Supplementary Table S8*) were strongly enriched for *KMT2A-r* target genes, and notably, many genes were known to be upregulated by KMT2A (*Online Supplementary Figure S6B*), which is in line with our hypothesis that limiting SAM results in suppressed MLL function and fits with the loss of activating histone marks. While H3K4 trimethylation was reduced at many of the key target genes previously highlighted (Figure 4H), some genes showed increased H3K4 trimethylation (*Online Supplementary Figure S6C*). ChaC glutathione-specific γ-glutamylcyclotransferase 1 (CHAC1), for example, a gene crucial for controlling cellular response to redox imbalance was the most affected,[30] which is in concordance with the increased expression observed upon MR in the transcriptomics data (*Online Supplementary Figure S6D*). These findings suggest that *KMT2A-r* leukemias require high SAM levels to maintain histone hypermethylation, a state unsustainable without methionine, ultimately leading to global histone methylation repression. Combined with other metabolic changes, this results in MR-induced cell death.

A drug screen reveals synergy between histone deacetylase inhibitors and MAT2A inhibitor FIDAS-5 in *KMT2A*-rearranged leukemia

Our results show that *KMT2A-r* leukemia strongly depends on methionine and SAM for proliferation and survival. This creates a vulnerability for this high-risk leukemia subset, which we demonstrated can be effectively targeted by restricting methionine dietarily or by disrupting the methionine cycle with FIDAS-5. We observed increased sensitivity to FIDAS-5 in *KMT2A-r* cell lines and PDX samples (Figure 3H; *Online Supplementary Figure S4E*), but were interested in finding drug combinations that could further potentiate these effects. We performed a drug screen in *KMT2A-r* SEM cells testing 241 different compounds, that are either used in pediatric oncology practice or are being tested in clinical studies, in combination with FIDAS-5 (*Online Supplementary Table S3*). Strikingly, six of the top 20 compounds found to bolster the effect of FIDAS-5 were histone deacetylase (HDAC) inhibitors, with fimepinostat and panobinostat being the top two hits (Figure 5A; *Online Supplementary Figure S7A*). Follow-up validation experiments confirmed this, indicating a clear synergistic response (Figure 5B). We next tested eight different primary *KMT2A-r* PDX samples with FIDAS-5 and fimepinostat *ex vivo* (Figure 5C). Using SynergyFinder,[31] we calculated zero interaction potency (ZIP) synergy scores and showed that in all but two of the patient samples tested, synergy could be identified (*Online Supplementary Figure S7B*), and no antagonism was found across the spectrum of the tested concentrations. Of note, one of the samples (PDX 8) was extremely sensitive to FIDAS-5 as monotherapy and an accurate synergy score could not be determined.

MAT2A inhibitor FIDAS-5 in combination with histone deacetylase inhibitor fimepinostat impairs *KMT2A*-rearranged leukemia progression

As a final validation, we tested this drug combination *in vivo*. We transplanted cells from PDX 1 10 days prior to starting treatment and orally administered FIDAS-5 (20 mg/kg), fimepinostat (75 mg), combination, or vehicle for 3 weeks (Figure 6A). Leukemia progression was monitored weekly, and mice were sacrificed when the tumor load exceeded 50% of the total leukocytes (*Online Supplementary Figure S8A*). Fimepinostat treatment alone did not significantly increase event-free survival (EFS), whereas FIDAS-5 treatment as single agent was effective, and the combination treatment even further increased EFS (Figure 6B). We used interpolated growth curve fitting to calculate the tumor load in the treated mice when control mice reached 50% tumor load (on average, 14.8 days after treatment initiation). Consistent with Kaplan-Meier analysis, the combination treatment was significantly synergistic and effectively hindered leukemia progression (Figure 6C). Importantly, both drugs were well-tolerated, with weight loss being the only

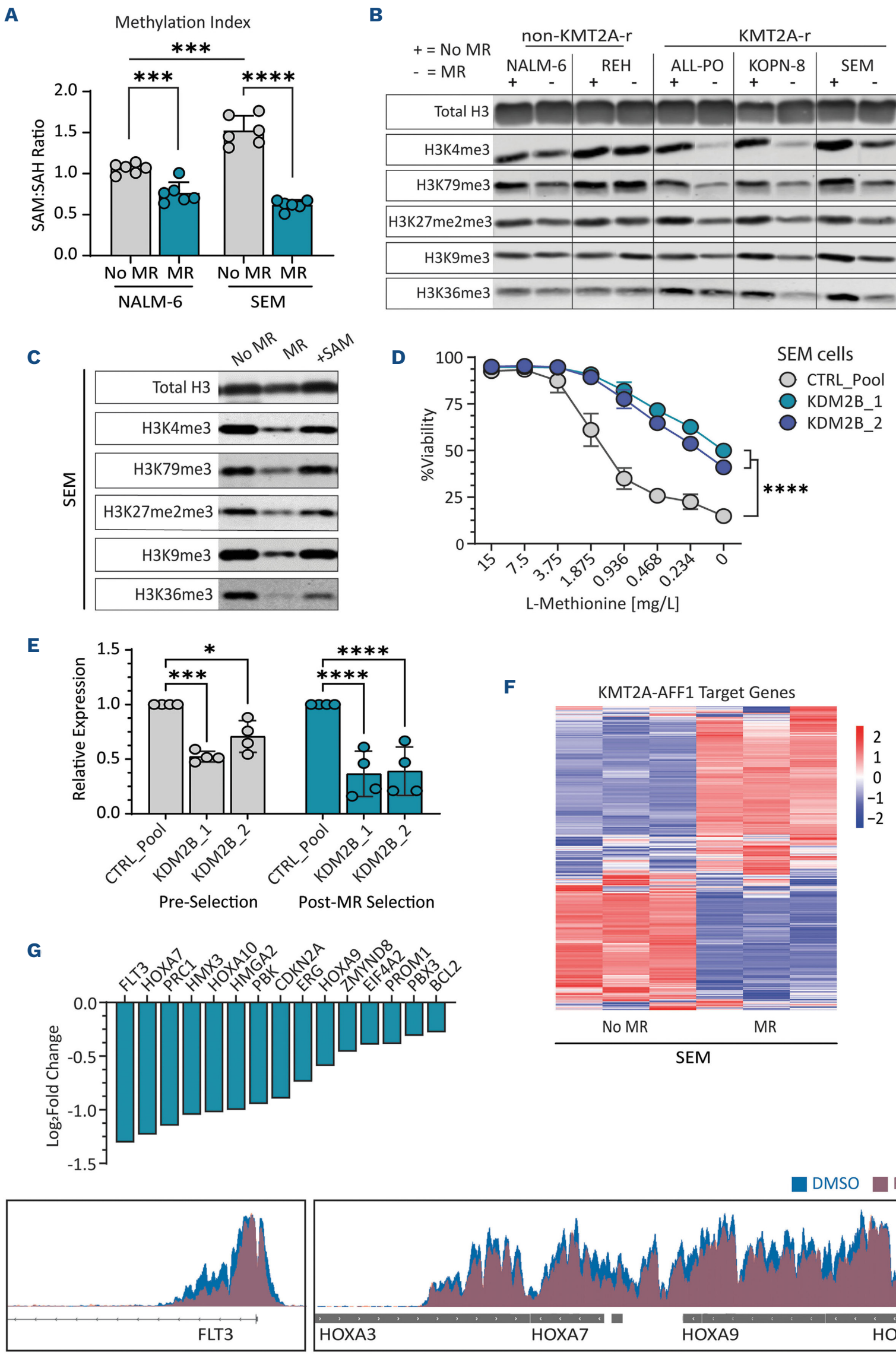

Continued on following page.

Figure 4. Methionine restriction triggers global suppression of histone methylation in *KMT2A*-rearranged leukemias, inducing rapid apoptosis. (A) Methylation index, indicated by the S-adenosylmethionine (SAM) to S-adenosylhomocysteine (SAH) ratio, in both NALM-6 and SEM cells before and after 24 hours (h) complete methionine depletion. *P* values were calculated using a two-way ANOVA and Šídák's multiple comparisons test (***P<0.001; ****P<0.0001). (B) Western blot of histone modifications (H3K4, H3K79, H3K27, H3K9, H3K36) and total histone 3 from lysates of B-cell progenitor acute lymphoblastic leukemia (BCP-ALL) cells treated for 48 h with complete methionine restriction (MR). (C) Western blot of histone modifications and total histone 3 from lysates of SEM cells treated for 48 h MR or 48 h MR with 10 μM S-adenosylmethionine (SAM) added back. (D) Dose response of *KDM2B* knockdown SEM cells (using 2 different hairpins) and control SEM cells (non-targeting small hairpin RNA) to decreasing levels of methionine in RPMI1640 medium. Results shown are the mean ± standard deviation (SD) from 3 independent experiments. *P* value was calculated using a one-way ANOVA of the area under the curves (AUC) and Dunnett's multiple comparisons test (****P<0.0001). (E) Relative *KDM2B* mRNA expression determined by quantitative polymerase chain reaction in *KDM2B* KD and control SEM cells before and after 7-day selection with MR medium. *P* value was calculated using a two-way ANOVA and Dunnett's multiple comparisons test (*P<0.05; ***P<0.001; ****P<0.0001). (F) Heatmap showing unsupervised clustering of expression obtained using RNA sequencing from a *KMT2A* gene signature in SEM cells before and after 24h MR. Signature is derived from *KMT2A-AFF1* target genes reported by Kerry *et al.*[29] (G) Log_2fold change in expression of specific *KMT2A-AFF1* target genes from the *KMT2A* gene signature, obtained using RNA sequencing. (H) Chromatin immunoprecipitation tracks showing the presence of H3K4 trimethylation at the same locus in dimethylsulfoxide (DMSO) control (blue) and FIDAS-5 treated (red) cells.

observed side effect caused by fimepinostat (*Online Supplementary Figure S8B*). To mitigate excessive weight loss, the fimepinostat dose was reduced to 25 mg/kg after the first week of treatment for the remainder of the experiment. We repeated the experiment using a second PDX sample (PDX 2) and added an additional treatment block (*Online Supplementary Figure S8C*). Prolonged treatment was well-tolerated, and weight loss was minimal with the optimized fimepinostat dose (*Online Supplementary Figure S8D*). Owing to the tissue trophism of this leukemia,[32] blood counts were uninformative. Using spleen weight as an indicator of tumor burden however, we noted that combination therapy resulted in nearly a 25% size reduction compared to control mice. Compared to mice treated with fimepinostat or FIDAS-5 alone, this was a greater reduction of 14% and 19%, respectively (Figure 6D). Our results strongly demonstrate that combined treatment with HDAC inhibitors and MAT2A inhibitors is cytotoxic for *KMT2A-r* ALL, both *in vitro* and *in vivo*.

Discussion

Metabolic reprogramming in cancer cells offers promising therapeutic opportunities to enhance leukemia treatment outcomes in high-risk subsets while minimizing treatment-related complications. We find that *KMT2A-r* leukemia is highly sensitive to MR and show a profound impact of MR on the metabolome and epigenome. Importantly, we provide proof of concept that dietary MR and pharmacological targeting of the methionine cycle impair lymphoblastic leukemia progression.

For infants and children suffering from *KMT2A-r* leukemia, dietary MR using Food and Drug Administration-approved methionine-free infant formula (Hominex®-1) or medical food (Hominex®-2), originally created for individuals with vitamin B6-non-responsive homocystinuria or hypermethioninemia, are feasible options. Two clinical trials were conducted, testing Hominex®-2 in glioblastoma and breast cancer patients, but were unfortunately terminated early due to low enrollment (*clincaltrials gov. Identifier: NCT03186937, NCT00508456*). A phase I clinical trial assessing the feasibility of a MR diet showed similar effects in adults, reporting a 58% reduction in plasma methionine levels after just 2 weeks on a controlled 90% MR diet. The diet was well-tolerated throughout the 16-week period, with weight loss being the sole reported side effect.[33] It is interesting to note that *KMT2A-r* cell lines derived from adults displayed reduced responsiveness compared to their pediatric counterparts in our experiments, suggesting that the cell-of-origin, which varies across age groups,[34] influences methionine dependency and suggests that infants may benefit more from a MR diet. Another intriguing therapeutic approach is enzymatic methionine depletion. Recombinant methioninase was first tested by intravenous injection but was found to cause anaphylaxis unless pegylated.[35] However, unlike recombinant asparaginase, pegylated methioninase still has a very short half-life *in vivo*.[36] Alternatively, oral administration of methioninase is well-tolerated and has demonstrated effectiveness in preclinical studies and human cases.[37-39]

Epigenetic remodeling driven by *KMT2A-r* fusion complexes is integral to leukemia formation in this subtype[40] and relies on SAM as methyl donor. Although other methylation processes, including protein and DNA methylation may also be affected, we attribute the sensitivity of *KMT2A-r* cells to MR to the profound effects on histone methylation that we observed. In our study, reducing the availability of SAM with FIDAS-5 treatment was more effective than the 95% MR diet *in vivo*. Preclinical studies in lung and colorectal cancer show antitumor efficacy of MAT2A inhibitors,[41,42] and phase I clinical trials are ongoing in MTAP-deleted solid tumors and lymphomas (*clincaltrials gov. Identifier: NCT03435250, NCT03435250*). Drugs interfering with the assembly or function of *KMT2A-r* fusion complexes, such as Disruptor of telomeric silencing 1-like (DOT1L) and Menin inhibitors, have also shown efficacy in preclinical models,[43,44] with Menin inhibitors showing

promise in ongoing clinical trials (*clinicaltrials gov. Identfier: NCT05153330, NCT05360160*). Somatic mutations in the *MENIN* gene can lead to clinical resistance however,[45] and other studies suggest that single-target epigenetic agents are insufficient and simultaneous targeting of different components of the *KMT2A*-complex could be more effective.[46] Recent work has shown how one-carbon metabolism can shape epigenetic regulation through histone methylation,[16,47] supporting our findings that MR impacts the *KMT2A-r* leukemia epigenome. We observed

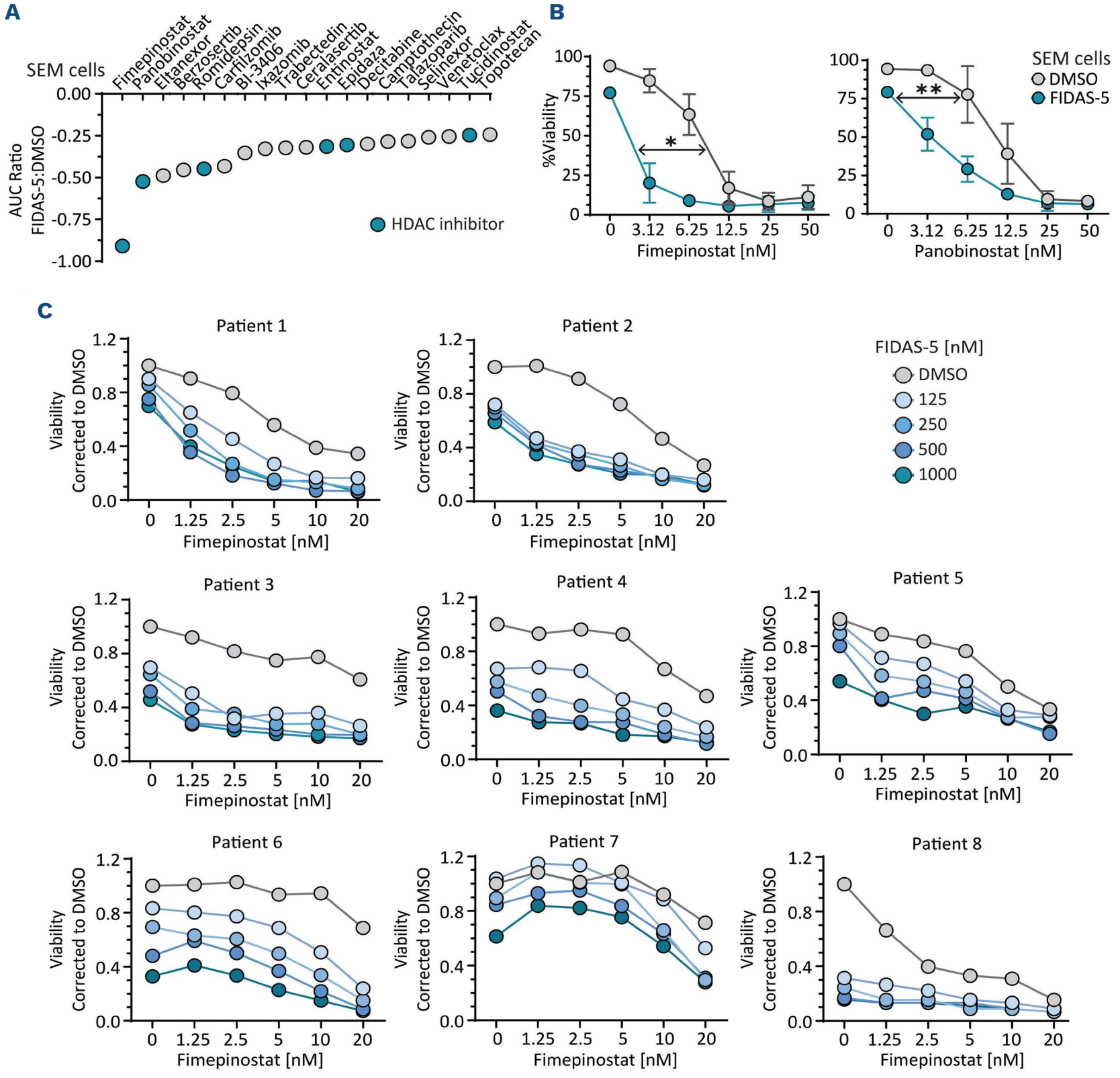

Figure 5. A drug screen reveals synergy between histone deacetylase inhibitors and methionine adenosyltransferase 2A inhibitor FIDAS-5 in *KMT2A*-rearranged leukemia. (A) A drug screen was performed with 241 different compounds either as single therapy (Ctrl) or in combination with 1 μM FIDAS-5 in SEM cells. Cell proliferation was measured after 72 hours (h) using an MTT assay. Separate area under the curves (AUC) were calculated for Ctrl and FIDAS-5 combination treated and the top 20 hits with an AUC ratio FIDAS-5 to Ctrl less than -0.25 were plotted. Histone deacetylase (HDAC) inhibitors are highlighted in blue. (B) Dose titration of the top two HDAC inhibitors fimepinostat and panobinostat in combination with 1 μM FIDAS-5. Cell viability was measured via flow cytometry after 72 h treatment. Results shown are the mean ± standard deviation (SD) from 3 independent experiments. *P* value was calculated using a one-way ANOVA of the AUC and Dunnett's multiple comparisons test (**P*<0.05; ***P*<0.01). (C) Eight different patient-derived xenografts (PDX) were tested *in vitro* with 5 doses of FIDAS-5 against 6 doses of fimepinostat in a synergy matrix. Cells were seeded on mesenchymal stem cells and treated for 72 h before measuring cell viability via flow cytometry. MAT2A: methionine adenosyltransferase 2A; *KMT2A-r*: *KMT2A*-rearranged; DMSO: dimethylsulfoxide.

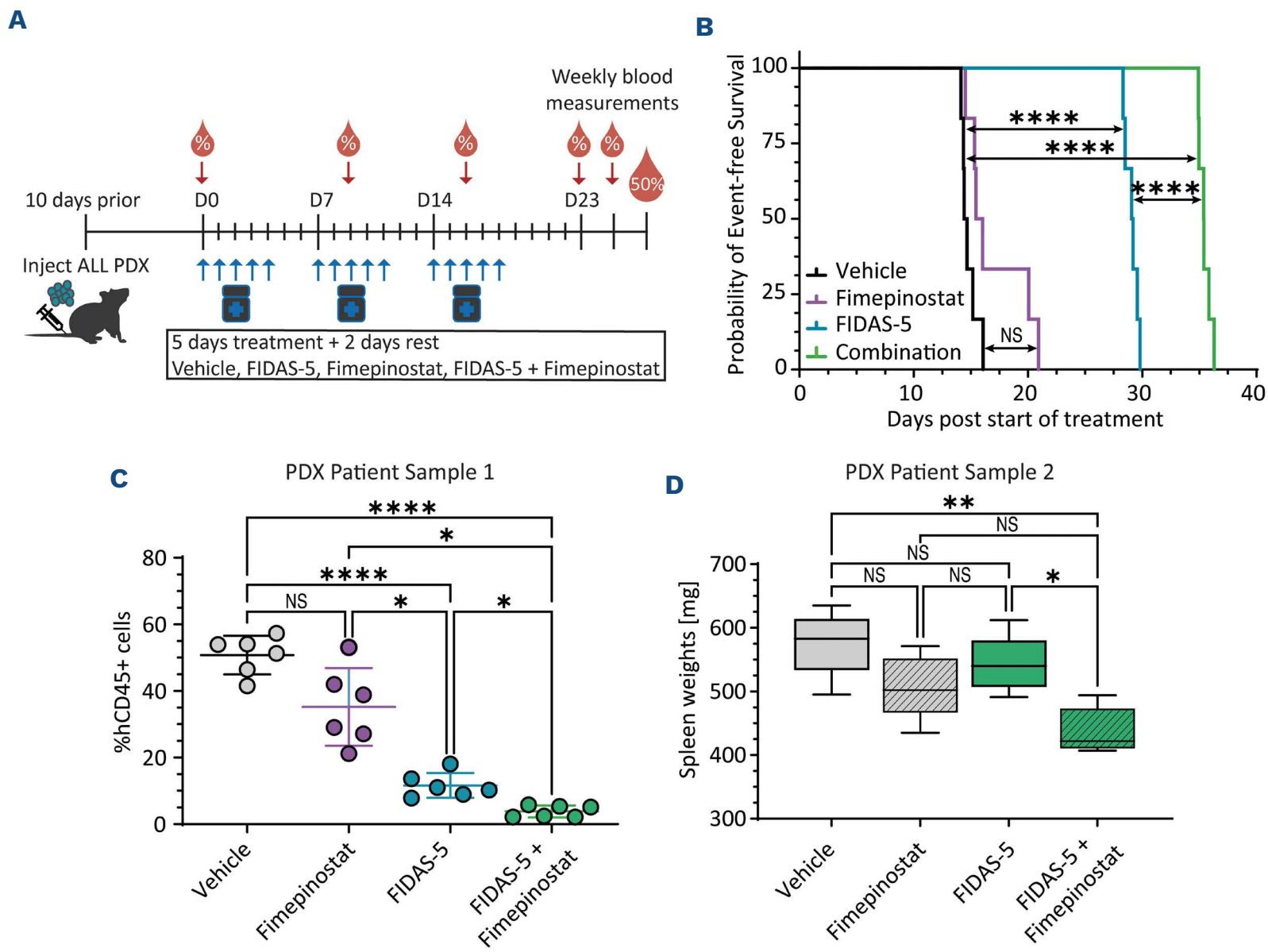

Figure 6. Methionine adenosyltransferase 2A inhibitor FIDAS-5 in combination with histone deacetylase inhibitor fimepinostat impairs *KMT2A*-rearranged leukemia progression. (A) Patient-derived xenograft (PDX) patient sample 1 was transplanted via intravenous injection 10 days prior to the start of treatment. Mice (N=24) were then randomized and given an oral vehicle, FIDAS-5 (20 mg/kg), fimepinostat, or combination dose for 3 weeks, with 5 consecutive days of treatment followed by 2 days of rest; 75 mg/kg of fimepinostat was administered the first week and reduced to 25 mg/kg the remaining 2 weeks. Tumor burden was monitored in peripheral blood via weekly flow cytometry measurements. (B) Kaplan-Meier survival analysis for each treatment group. *P* values were calculated using a one-way ANOVA and Tukey's multiple comparisons test (****P<0.0001). (C) The projected tumor load for each mouse on day 14.8, which was the average interpolated time it took control mice to reach 50% leukemic blasts. *P* values were calculated using a Brown-Forsythe and Welch one-way ANOVA and Dunnett's multiple comparisons test (*P<0.05; ****P<0.0001). (D) Weights of the spleens from engrafted PDX patient sample 2, obtained 60 days after transplantation. *P* values were calculated using a Brown-Forsythe and Welch one-way ANOVA and Dunnett's multiple comparisons test (*P<0.05; **P<0.01). NS: not significant.

global suppression of histone methylation, which in turn affects the *KMT2A* gene signature and causes deactivation of several target genes essential for proliferation and survival. This suggests that Menin and DOT1L inhibitors converge on the same pathway. Although we find no evidence of DOT1L suppression in our models, others have shown that MR results in downregulation of DOT1L expression in *KMT2A-r* cells.[48] Of note, while in AML the effects of MR can be phenocopied by inhibition of the methyltransferase SETD2, this is not the case in ALL, indicating lineage-dependent differences in epigenetic regulation.[16] Combining Menin or DOT1L inhibitors with MR is an interesting avenue for further investigation. Although in preliminary *in vitro* experiments we find no synergistic effects (*data not shown*), combining partial MR with Menin and/or DOT1L inhibition *in vivo* may result in enhanced therapeutic efficacy.

Exploiting epigenetic vulnerabilities in *KMT2A-r* leukemia and sensitizing cells to metabolic stressors extends beyond targeting the fusion complex. We demonstrate that co-inhibiting HDAC and MAT2A is highly cytotoxic and effectively slows leukemic growth *in vivo*. Although the molecular mechanism underlying this drug interaction remains to be determined, HDAC inhibitors were previously described to selectively induce cell death in *KMT2A-r* ALL cells by repressing histone 2B (H2B) ubiquitination. This process is required for H3K79 and H3K4 methylation, important modifications associated with the *KMT2A* gene signature.[49] Interestingly in this study, while HDAC inhibition reduced H2B ubiquitination, global

H3K79 and H3K4 methylation were not strongly affected. This was consistent with another study showing that loss of H2B ubiquitination results in focal, rather than global, demethylation.[50] Therefore the combined effect of HDAC and MAT2A inhibition might be attributable to the global demethylation effects of reduced SAM levels, which complement the apparent limitations of HDAC inhibition alone. With five approved HDAC inhibitors and over 20 in clinical evaluation, these agents hold significant potential for the treatment of hematological malignancies.[51,52] Inhibition of class 1 HDAC induces apoptosis in BCP-ALL cells,[53] and panobinostat, a pan-HDAC inhibitor approved for multiple myeloma, significantly impairs *KMT2A-r* leukemia growth.[49] Fimepinostat, the dual pan-HDAC and phosphatidylinositol 3-kinase (PI3K) inhibitor used in this study, demonstrated preclinical efficacy in several hematological malignancies,[54-56] and is well-tolerated in phase I trials in patients with refractory lymphoma, multiple myeloma, and DLBCL.[57] Multiple ongoing trials, including those in young adults and children, are assessing the potential of these inhibitors (*clinicaltrials gov. Identifier: NCT03893487, NCT02909777, NCT02307240, NCT03002623*). *KMT2A-r* leukemia, especially in infants, exhibits a low mutational burden with few somatic mutations. However, activated PI3K/RAS signaling has been reported in *KMT2A-r* ALL cases and is suggested to confer a growth advantage.[19] Our study prompts further exploration of PI3K inhibition, though we attribute much of the observed effects to HDAC inhibition. This is supported by the fact that other HDAC inhibitors were identified to synergize with MAT2A inhibition in our drug screen, while other PI3K inhibitors were not.

Metabolomic and transcriptomic analyses reveal that differential sensitivity to MR is largely metabolically driven. We find distinct differences between cell lines both basally and post-MR, suggesting that non-*KMT2A-r* leukemic cells have greater metabolic plasticity and may adapt better to amino acid stress than *KMT2A-r* cells. Our findings suggest that *KMT2A-r* SEM cells rely more heavily on *de novo* pyrimidine synthesis, presenting an interesting opportunity for combination therapy with MR and DHODH inhibition. This essential enzyme in the *de novo* pyrimidine synthesis pathway has been implicated as a target to induce differentiation[58] and slow growth in hematological malignancies.[59] Although several DHODH inhibitors have been clinically evaluated, none have received approval for cancer treatment due to insufficient single-agent effectivity. A potential limitation of solely targeting DHODH is that cells can alternatively source nucleotides from the salvage pathway. This could be resolved with MR, as it broadly affects both *de novo* and salvage mechanisms in purine and pyrimidine synthesis, and dietary MR has already been reported to synergize with nucleotide synthesis inhibition in cancer.[10,60]

Finally, it is important to keep in mind the effect of MR on the immune system. Activated T cells demand more glucose, leucine, and arginine[61] and use enhanced glucose metabolism and lipid biosynthesis for clonal expansion and differentiation.[62] T-cell activation induces mitochondrial reprogramming, further stimulating the one-carbon cycle,[63] and methionine metabolism influences helper T-cell effector responses.[64] The potential consequences of MR on the immune system should be carefully considered when combined with immunotherapies such as blinatumomab or chimeric antigen receptor T cells for ALL. In contrast, tumor methionine metabolism can also drive T-cell exhaustion, and perturbation of the methionine cycle may protect against and prevent exhaustion.[65] A recent study also demonstrated that chimeric antigen receptor T cells can be re-engineered to express transmembrane amino acid transporters, making them more competitive in the tumor microenvironment.[66] Although methionine metabolism is vital for normal immune function, emerging evidence suggests that intervening with the methionine cycle could boost immune responses, further broadening the versatility of MR as a therapy.

Disclosures

No conflicts of interest to disclose.

Contributions

TT, LTvdM and FVL conceptualized the study. TT, TJJR, SW, WZ, MR, DvIW, BMTV, MB, PS, DH and LTvdM performed experiments and analyzed the data. KJTG, RH, and JB-H performed bio-informatic and statistical analyses, NMV-D supervised and interpreted metabolomic analysis, TT, LTvdM and FVL wrote the manuscript, which was edited and approved by all authors.

Acknowledgments

We would like to acknowledge the High Throughput Screening center, specifically Selma Eising, Vicky Amo-Addae, and Jan Molenaar, at the Princess Máxima Center for their help in performing the drug screen. We want to thank the staff of the PRIME-unit at the Radboud University Animal Research Facility for their help, namely Karin de Haas-Cremers, Bianca Lemmers-van de Weem, Kitty Lemmens-Hermans, and Floor Moonen, with the in vivo studies. And we would also like to thank Prof. R. Kuiper and Prof. O. Heidenreich for their critical feedback on the manuscript and help along the way.

Funding

This work was supported by research funding from the Dutch Cancer Society (KWF) (grant #11249)

Data-sharing statement

RNA sequencing and ChIP-seq data can be found in the Gene Expression Omnibus Repository (GSE234806). For other raw data, R scripts, and/or protocols please contact the corresponding author.

References

1. Pieters R, De Lorenzo P, Ancliffe P, et al. Outcome of infants younger than 1 year with acute lymphoblastic leukemia treated with the interfant-06 protocol: results from an international phase III randomized study. J Clin Oncol. 2019;37(25):2246-2256.
2. Sun YN, Hu YX, Gao L, et al. The therapeutic efficacy of pediatric ALL patients with MLL gene rearrangement treated with CCLG-ALL2008 protocol. Eur Rev Med Pharmacol Sci. 2018;22(18):6020-6029.
3. Tosta Perez M, Herrera Belen L, Letelier P, et al. L-asparaginase as the gold standard in the treatment of acute lymphoblastic leukemia: a comprehensive review. Med Oncol. 2023;40(5):150.
4. Butler M, van der Meer LT, van Leeuwen FN. Amino acid depletion therapies: starving cancer cells to death. Trends Endocrinol Metab. 2021;32(6):367-381.
5. Sivanand S, Vander Heiden MG. Emerging roles for branched-chain amino acid metabolism in cancer. Cancer Cell. 2020;37(2):147-156.
6. Yoo HC, Park SJ, Nam M, et al. A variant of SLC1A5 is a mitochondrial glutamine transporter for metabolic reprogramming in cancer cells. Cell Metab. 2020;31(2):267-283.e12.
7. Cavuoto P, Fenech MF. A review of methionine dependency and the role of methionine restriction in cancer growth control and life-span extension. Cancer Treat Rev. 2012;38(6):726-736.
8. Sharma B, Singh S, Kanwar SS. L-methionase: a therapeutic enzyme to treat malignancies. Biomed Res Int. 2014;2014:506287.
9. Jeon H, Kim JH, Lee E, et al. Methionine deprivation suppresses triple-negative breast cancer metastasis in vitro and in vivo. Oncotarget. 2016;7(41):67223-67234.
10. Gao X, Sanderson SM, Dai Z, et al. Dietary methionine influences therapy in mouse cancer models and alters human metabolism. Nature. 2019;572(7769):397-401.
11. Krivtsov AV, Armstrong SA. MLL translocations, histone modifications and leukaemia stem-cell development. Nat Rev Cancer. 2007;7(11):823-833.
12. Butler M, van Ingen Schenau DS, Yu J, et al. BTK inhibition sensitizes acute lymphoblastic leukemia to asparaginase by suppressing the amino acid response pathway. Blood. 2021;138(23):2383-2395.
13. Pang Z, Chong J, Zhou G, et al. MetaboAnalyst 5.0: narrowing the gap between raw spectra and functional insights. Nucleic Acids Res. 2021;49(W1):W388-W396.
14. Kanehisa M, Goto S. KEGG: kyoto encyclopedia of genes and genomes. Nucleic Acids Res. 2000;28(1):27-30.
15. Prinsen H, Schiebergen-Bronkhorst BGM, Roeleveld MW, et al. Rapid quantification of underivatized amino acids in plasma by hydrophilic interaction liquid chromatography (HILIC) coupled with tandem mass-spectrometry. J Inherit Metab Dis. 2016;39(5):651-660.
16. Cunningham A, Erdem A, Alshamleh I, et al. Dietary methionine starvation impairs acute myeloid leukemia progression. Blood. 2022;140(19):2037-2052.
17. Shuvalov O, Petukhov A, Daks A, et al. One-carbon metabolism and nucleotide biosynthesis as attractive targets for anticancer therapy. Oncotarget. 2017;8(14):23955-23977.
18. So J, Lewis AC, Smith LK, et al. Inhibition of pyrimidine biosynthesis targets protein translation in acute myeloid leukemia. EMBO Mol Med. 2022;14(7):e15203.
19. Andersson AK, Ma J, Wang J, et al. The landscape of somatic mutations in infant MLL-rearranged acute lymphoblastic leukemias. Nat Genet. 2015;47(4):330-337.
20. Locasale JW. Serine, glycine and one-carbon units: cancer metabolism in full circle. Nat Rev Cancer. 2013;13(8):572-583.
21. Struck AW, Thompson ML, Wong LS, Micklefield J. S-adenosyl-methionine-dependent methyltransferases: highly versatile enzymes in biocatalysis, biosynthesis and other biotechnological applications. Chembiochem. 2012;13(18):2642-2655.
22. Zhu L, Li Q, Wong SH, et al. ASH1L links histone H3 lysine 36 dimethylation to MLL leukemia. Cancer Discov. 2016;6(7):770-783.
23. Bu J, Chen A, Yan X, et al. SETD2-mediated crosstalk between H3K36me3 and H3K79me2 in MLL-rearranged leukemia. Leukemia. 2018;32(4):890-899.
24. He J, Nguyen AT, Zhang Y. KDM2b/JHDM1b, an H3K36me2-specific demethylase, is required for initiation and maintenance of acute myeloid leukemia. Blood. 2011;117(14):3869-3880.
25. Martin C, Zhang Y. The diverse functions of histone lysine methylation. Nat Rev Mol Cell Biol. 2005;6(11):838-849.
26. Janzer A, Stamm K, Becker A, et al. The H3K4me3 histone demethylase Fbxl10 is a regulator of chemokine expression, cellular morphology, and the metabolome of fibroblasts. J Biol Chem. 2012;287(37):30984-30992.
27. Kang JY, Park JW, Hahm JY, Jung H, Seo SB. Histone H3K79 demethylation by KDM2B facilitates proper DNA replication through PCNA dissociation from chromatin. Cell Prolif. 2020;53(11):e12920.
28. Berry WL, Janknecht R. KDM4/JMJD2 histone demethylases: epigenetic regulators in cancer cells. Cancer Res. 2013;73(10):2936-2942.
29. Kerry J, Godfrey L, Repapi E, et al. MLL-AF4 spreading identifies binding sites that are distinct from super-enhancers and that govern sensitivity to DOT1L inhibition in leukemia. Cell Rep. 2017;18(2):482-495.
30. Sun J, Ren H, Wang J, et al. CHAC1: a master regulator of oxidative stress and ferroptosis in human diseases and cancers. Front Cell Dev Biol. 2024;12:1458716.
31. Ianevski A, Giri AK, Aittokallio T. SynergyFinder 3.0: an interactive analysis and consensus interpretation of multi-drug synergies across multiple samples. Nucleic Acids Res. 2022;50(W1):W739-W743.
32. Akinduro O, Weber TS, Ang H, et al. Proliferation dynamics of acute myeloid leukaemia and haematopoietic progenitors competing for bone marrow space. Nat Commun. 2018;9(1):519.
33. Epner DE, Morrow S, Wilcox M, Houghton JL. Nutrient intake and nutritional indexes in adults with metastatic cancer on a phase I clinical trial of dietary methionine restriction. Nutr Cancer. 2002;42(2):158-166.
34. le Viseur C, Hotfilder M, Bomken S, et al. In childhood acute lymphoblastic leukemia, blasts at different stages of immunophenotypic maturation have stem cell properties. Cancer Cell. 2008;14(1):47-58.
35. Yang Z, Wang J, Yoshioka T, et al. Pharmacokinetics, methionine depletion, and antigenicity of recombinant methioninase in primates. Clin Cancer Res. 2004;10(6):2131-2138.
36. Yang Z, Sun X, Li S, et al. Circulating half-life of PEGylated recombinant methioninase holoenzyme is highly dose dependent on cofactor pyridoxal-5'-phosphate.

Cancer Res. 2004;64(16):5775-5778.
37. Kubota Y, Han Q, Hozumi C, et al. Stage IV pancreatic cancer patient treated with folfirinox combined with oral methioninase: a highly-rare case with long-term stable disease. Anticancer Res. 2022;42(5):2567-2572.
38. Kubota Y, Han Q, Hamada K, et al. Long-term stable disease in a rectal-cancer patient treated by methionine restriction with oral recombinant methioninase and a low-methionine diet. Anticancer Res. 2022;42(8):3857-3861.
39. Lim HI, Yamamoto J, Han Q, et al. Response of triple-negative breast cancer liver metastasis to oral recombinant methioninase in a patient-derived orthotopic xenograft (PDOX) model. In Vivo. 2020;34(6):3163-3169.
40. de Barrios O, Parra M. Epigenetic control of infant B cell precursor acute lymphoblastic leukemia. Int J Mol Sci. 2021;22(6):3127.
41. Zhang W, Sviripa V, Chen X, et al. Fluorinated N,N-dialkylaminostilbenes repress colon cancer by targeting methionine S-adenosyltransferase 2A. ACS Chem Biol. 2013;8(4):796-803.
42. Kalev P, Hyer ML, Gross S, et al. MAT2A inhibition blocks the growth of MTAP-deleted cancer cells by reducing PRMT5-dependent mRNA splicing and inducing DNA damage. Cancer Cell. 2021;39(2):209-224.e11.
43. Perner F, Gadrey JY, Xiong Y, et al. Novel inhibitors of the histone methyltransferase DOT1L show potent antileukemic activity in patient-derived xenografts. Blood. 2020;136(17):1983-1988.
44. Krivtsov AV, Evans K, Gadrey JY, et al. A Menin-MLL inhibitor induces specific chromatin changes and eradicates disease in models of MLL-rearranged leukemia. Cancer Cell. 2019;36(6):660-673.e11.
45. Perner F, Stein EM, Wenge DV, et al. MEN1 mutations mediate clinical resistance to menin inhibition. Nature. 2023;615(7954):913-919.
46. Dafflon C, Craig VJ, Mereau H, et al. Complementary activities of DOT1L and Menin inhibitors in MLL-rearranged leukemia. Leukemia. 2017;31(6):1269-1277.
47. Bian Y, Li W, Kremer DM, et al. Cancer SLC43A2 alters T cell methionine metabolism and histone methylation. Nature. 2020;585(7824):277-282.
48. Barve A, Vega A, Shah PP, et al. Perturbation of methionine/S-adenosylmethionine metabolism as a novel vulnerability in MLL rearranged leukemia. Cells. 2019;8(11):1322.
49. Garrido Castro P, van Roon EHJ, Pinhancos SS, et al. The HDAC inhibitor panobinostat (LBH589) exerts in vivo anti-leukaemic activity against MLL-rearranged acute lymphoblastic leukaemia and involves the RNF20/RNF40/WAC-H2B ubiquitination axis. Leukemia. 2018;32(2):323-331.
50. Lee JS, Shukla A, Schneider J, et al. Histone crosstalk between H2B monoubiquitination and H3 methylation mediated by COMPASS. Cell. 2007;131(6):1084-1096.
51. Bondarev AD, Attwood MM, Jonsson J, et al. Recent developments of HDAC inhibitors: emerging indications and novel molecules. Br J Clin Pharmacol. 2021;87(12):4577-4597.
52. Vega-Garcia N, Malatesta R, Estella C, et al. Paediatric patients with acute leukaemia and KMT2A (MLL) rearrangement show a distinctive expression pattern of histone deacetylases. Br J Haematol. 2018;182(4):542-553.
53. Stubbs MC, Kim W, Bariteau M, et al. Selective inhibition of HDAC1 and HDAC2 as a potential therapeutic option for B-ALL. Clin Cancer Res. 2015;21(10):2348-2358.
54. Mondello P, Derenzini E, Asgari Z, et al. Dual inhibition of histone deacetylases and phosphoinositide 3-kinase enhances therapeutic activity against B cell lymphoma. Oncotarget. 2017;8(8):14017-14028.
55. Chen Y, Peubez C, Smith V, et al. CUDC-907 blocks multiple pro-survival signals and abrogates microenvironment protection in CLL. J Cell Mol Med. 2019;23(1):340-348.
56. Li X, Su Y, Madlambayan G, et al. Antileukemic activity and mechanism of action of the novel PI3K and histone deacetylase dual inhibitor CUDC-907 in acute myeloid leukemia. Haematologica. 2019;104(11):2225-2240.
57. Oki Y, Kelly KR, Flinn I, et al. CUDC-907 in relapsed/refractory diffuse large B-cell lymphoma, including patients with MYC-alterations: results from an expanded phase I trial. Haematologica. 2017;102(11):1923-1930.
58. Sykes DB, Kfoury YS, Mercier FE, et al. Inhibition of dihydroorotate dehydrogenase overcomes differentiation blockade in acute myeloid leukemia. Cell. 2016;167(1):171-186.e15.
59. Mao C, Liu X, Zhang Y, et al. DHODH-mediated ferroptosis defence is a targetable vulnerability in cancer. Nature. 2021;593(7860):586-590.
60. Chaturvedi S, Hoffman RM, Bertino JR. Exploiting methionine restriction for cancer treatment. Biochem Pharmacol. 2018;154:170-173.
61. Kidani Y, Elsaesser H, Hock MB, et al. Sterol regulatory element-binding proteins are essential for the metabolic programming of effector T cells and adaptive immunity. Nat Immunol. 2013;14(5):489-499.
62. Swamy M, Pathak S, Grzes KM, et al. Glucose and glutamine fuel protein O-GlcNAcylation to control T cell self-renewal and malignancy. Nat Immunol. 2016;17(6):712-720.
63. Ron-Harel N, Santos D, Ghergurovich JM, et al. Mitochondrial biogenesis and proteome remodeling promote one-carbon metabolism for T cell activation. Cell Metab. 2016;24(1):104-117.
64. Roy DG, Chen J, Mamane V, et al. Methionine metabolism shapes T helper cell responses through regulation of epigenetic reprogramming. Cell Metab. 2020;31(2):250-266.e9.
65. Hung MH, Lee JS, Ma C, et al. Tumor methionine metabolism drives T-cell exhaustion in hepatocellular carcinoma. Nat Commun. 2021;12(1):1455.
66. Panetti S, McJannett N, Fultang L, et al. Engineering amino acid uptake or catabolism promotes CAR T-cell adaption to the tumor environment. Blood Adv. 2023;7(9):1754-1761.